Structural Study of the Thermally Induced and Photoinduced Phase Transitions of the 1,3,5-Trithia-2,4,6-triazapentalenyl (TTTA) Radical

Panče Naumov,*,†,‡,§ Jonathan P. Hill,†,|| Kenji Sakurai,⊥ Masahiko Tanaka,# and Katsuhiko Ariga||

International Center for Young Scientists, National Institute for Materials Science, 1-1 Namiki, Tsukuba, Ibaraki 305-0044, Japan, Institute of Chemistry, Faculty of Science, Sts. Cyril and Methodius University, POB 162, MK−1000 Skopje, Macedonia, Frontier Research Base for Global Young Researchers, Graduate School of Engineering, Osaka University, 2-1 Yamada-oka, Osaka, 565-0871 Suita, Japan, Supermolecules Group, National Institute for Materials Science, 1-1 Namiki, Tsukuba, Ibaraki 305-0044, Japan, Quantum Beam Center, National Institute for Materials Science, 1-2-1 Sengen, Tsukuba, Ibaraki 305-0047, Japan, and WEBRAM, SPring-8, National Institute for Materials Science, 1-1-1 Kouto, Mikazuki, Sayo, Hyogo 679-5198, Japan

Received: April 11, 2007; In Final Form: May 14, 2007

We report on the first direct atomic-level photodiffraction evidence for domain formation by doping with charge photocarriers of the stable organic radical TTTA (1,3,5-trithia-2,4,6-triazapentalenyl), which exhibits unusually wide thermal hysteresis of the paramagnetic-to-diamagnetic phase transition around ambient temperature. A setup for steady-state powder photodiffraction was developed for the purpose, composed of a second harmonic pulsed visible pump (532 nm) coupled with a powder diffractometer using monochromatic synchrotron X-ray radiation as the probe. The refined structures of the photoinduced phase and the high-temperature phase are structurally identical. The result supports the model according to which photoexcitation causes suppression of the spin-Peierls instability and separation of the radical dimers, resulting in a structure that is essentially identical with the unperturbed high-temperature phase.

1. Introduction

There is much scientific interest in stable organic radicals capable of reversible phase transitions because of the possibility of externally controlling the spin state of their free electrons, in addition to their crystal structure and other physical properties, such as the optical absorption spectrum and electric conductivity. The unshared electron can adopt one of the two possible spin states, thereby increasing the number of degrees of freedom and the overall multistability of the phase diagram by phases that differ in their spin ordering. Moreover, the free electrons contribute with a permanent magnetic moment, which can be conveniently coupled with external electromagnetic radiation and employed as a sensitive indicator of the phase state and composition of the material. Occasionally, the stable solid radicals act as strongly correlated systems, thus opening the possibility for controlling the collective structural properties of macroscopic domains in their structure by introducing localized structural perturbations with external stimuli, such as by increasing the average kinetic energy through heating or by seeding with defect sites by photoexcitation. Similar to the known electronically coupled closed-shell molecular systems, activation of cooperative mechanisms in such cases is expected to result in very high efficiency and ultrafast time response of switching of the opto-magneto-electro-structural properties of the material. If combined with the change of the spin state, these exotic properties offer powerful potential for applications, particularly in ultrafast spintronics, in the future.[1,2]

In principle, the enhanced conducting properties of organic open-shell systems could be conveniently realized by using stacks of strongly electronically interacting small, planar, stable radical molecules.[3−7] One of the most serious drawbacks of using planar radicals for switching the conductivity is their tendency for dimerization under ambient conditions, usually caused by Peierls instability of the one-dimensional (1D) radical chains. The dimerization results in alternating short and long contacts between neighboring molecules and a gap between the bonding and antibonding orbitals of the half-filled band, which ultimately renders the system semiconducting or insulating.[8,9] Efforts have been made to overcome this difficulty, mostly based on attempts to compensate for the *intra*columnar Peierls instability by increasing the *inter*columnar interactions or by stretching the bonding and antibonding bands to partially overlap through replacement of the sulfur with selenium atoms. However, attempts to prevent the dimerization proved only partially successful, until a few examples of thiazyl radicals that remain monomeric under ambient conditions were discovered. Among these, the 1,3,5-trithia-2,4,6-triazapentalenyl (TTTA) radical[10−12] is exceptional for several reasons: (1) It is stable in air and remains monomeric even at ambient temperature and pressure, down to about 230 K. (2) It shows bistability between two stable phases around ambient temperature, which is important for applications. (3) It shows an exceptionally wide hysteresis gap of about 80 K of the phase transition, thus enabling exploration of the region of bistability within a large temperature interval. (4) The two phases of TTTA have distinctly different structural,

* Corresponding author. E-mail: naumov.pance@nims.go.jp.
† International Center for Young Scientists, National Institute for Materials Science.
‡ Sts. Cyril and Methodius University.
§ Osaka University.
|| Supermolecules Group, National Institute for Materials Science.
⊥ Quantum Beam Center, National Institute for Materials Science.
SPring-8, National Institute for Materials Science.

10.1021/jp072807k CCC: $37.00
Published on Web 06/20/2007

optical, and magnetic properties.[11−13] (5) The compound can be deposited as a thin film on a metal substrate, enabling its properties as film and in bulk crystals to be studied and compared.[14] (6) The temperature of the thermal phase transition of TTTA can be controlled by applying pressure.[15] (7) TTTA is the only reported radical for which unidirectional phase switching by excitation with pulsed laser has been reported,[16] a property which may allow the phase composition to be controlled with visible light. In practice, however, the tendency of solid TTTA to undergo spontaneous sublimation under ambient conditions, an important aspect that has not been pointed out in the previous works on this compound, may cause problems in practical applications. In spite of this difficulty, TTTA has been one of the most studied thiazyl radicals. In the course of studying a model system of the multistability of strongly correlated organic molecules for designing radical-based room-temperature switching materials, it is very important to unravel the detailed mechanism of the thermal transitions and particularly of the photoinduced phase transition of TTTA, and to determine the exact structures of the phases involved.

The transition between the high-temperature (HT) paramagnetic and low-temperature (LT) diamagnetic lattices of TTTA proceeds through a reversible spin-Peierls (SP) $\pi-\pi$ dimerization of the stacked $S = 1/2$ molecules within the 1D radical chains.[11−13] Recently, Okamoto et al.[16] reported that the phase transition of the LT phase can also be induced by pulsed excitation and yields a third, photoinduced (PI) phase. Detailed spectroscopic study of the variation of the photoyield with the photon flux and the intensity of the incident laser excitation unraveled that the photoconversion of TTTA exhibits a threshold-like behavior, which is one of the main indications of a cooperatively driven process. It has been suggested that a critical concentration of photoinduced charge carriers, which in the case of TTTA probably exist as spinless charged solitons, can suppress the spin-Peierls instability acquired by the system by switching from the HT to the LT phase.[16] The resulting destabilization of the LT dimers triggers transition to the PI phase.

The effect of pulsed laser radiation on the structure of the LT phase of TTTA has been previously studied with polarized Raman spectroscopy at 296 and 11 K.[16] At both temperatures, the frequency shift of a band assigned to the characteristic Raman-active ν(CN) mode of the LT phase was observed. In general, although vibrational spectroscopy is very informative about the distribution of molecular energy over the vibrational modes, the interpretation of the spectra usually relies on (oftentimes semiempirical) band assignments subject to solid-state effects, and thus, they are not entirely conclusive about the actual molecular structure and geometry. Therefore, the similarity or eventual identity between the structures of PI and HT phases of TTTA could not be confirmed by the spectroscopic results. The diffraction methods, mainly X-ray diffraction, provide the most direct and precise information on the structure and molecular geometry with atomic level resolution. With X-rays, one can nondestructively probe the surface (scattering) as well as the bulk (diffraction) of single crystalline as well as microcrystalline (powder) samples. By monitoring fine changes of the electron density distribution accompanying chemical reactions or physical processes, it is possible to achieve direct observation of the alterations of the geometry during dynamical processes in the solid state, including phase transitions. Contrary to many thermally induced phase transitions, there are only a few photoinduced structural phase transitions that have been studied by diffraction methods.

Here, we report on the direct observation of the three phases of TTTA and an *in situ* study of the transition processes among its phases. By employing a special technique that combines powder diffraction with synchrotron X-rays and pulsed laser radiation, we have succeeded in complete structural characterization, with atomic level resolution, of the thermally induced phases and of the previously uncharacterized photoinduced phase. The results provide a qualitatively new insight into the behavior of TTTA in the solid state and help explain the mechanism of its phase transitions. The results also represent the first direct evidence of photoinduced suppression of SP instability in an organic radical crystal, showing that a combination of powder diffraction and light irradiation is a prospective technique for obtaining direct, atomic resolution information about the photoreactions or phase transitions in the solid state.

2. Experimental Procedures

2.1. Synthesis. Two synthetic procedures,[10,12] differing in the procedure for preparing the precursor chloride salt, have been reported for the synthesis of TTTA. In our hands, the original procedure of Wolmershäuser and Johann[10] gave smaller yields, necessitating some minor modifications. The following modifications were made during the synthesis of TTTA: In the initial reaction between sodium sulfide and 4,5-dichloro-1,2,5-thiadiazole, the reaction mixture was stirred at 313 K for 2 h followed by evaporation and extraction of the solid with anhydrous ethanol (2×15 mL). Following chlorination of the product of the initial reaction, the CCl_4 solution was filtered rather than being subjected to centrifugation. The compound was purified by sublimation with gradual heating under moderate vacuum obtained with a rotary pump (the pressure was not controlled). Overheating of the sample or poor vacuum led to a green decomposition product. Contrary to the mixture of phases observed before,[12] our sublimation experiments always resulted in the pure monoclinic phase.

2.2. ESR Spectra. The ESR spectra were recorded in a temperature-controlled cell with an EMX-Plus ESR spectrometer (Bruker Biospin) at the microwave frequency of 9.284 GHz and power of 0.5 mW, with a modulation amplitude of 2 G.

2.3. Single-Crystal Diffraction Analysis. Single-crystal X-ray diffraction data were collected[17] in ω-oscillation mode with a Bruker three-circle diffractometer equipped with a CCD detector and a combined He−N_2 open type LT system, using monochromatized laboratory X-ray radiation (Mo$K\alpha$, 0.71073 Å). The structures were solved using direct methods[18] and refined as anisotropic models without constraints on F^2.[19]

2.4. Powder Diffraction Analysis. The powder diffraction patterns were recorded in the 2Θ region of 0−65° at the undulator beamline BL15XU of SPring-8, the 8 GeV synchrotron in Harima (Japan), using a curved IP detector ($l = 400$ mm; resolution, 0.01°). The sample, loaded in a Ø0.3 mm Lindemann capillary and spun at 1 s^{-1}, was exposed for 5 s to X-rays of $\lambda = 0.6358$ Å (checked against silicon). The zero point was detected by exposure to the direct beam. Three patterns were averaged for each temperature point, and the averaged background of an empty capillary was subtracted from the averaged pattern. The structures were refined with RIETAN-2000.[20] The profiles were fitted with asymmetric pseudo-Voigt functions combining three Gaussian and four Lorentzian FWHM variables. The background was initially refined as a 12-variable function using the incremental Marquardt least-squares method and was kept fixed at the final refinement stages. Either anisotropic or isotropic thermal parameters were assigned to all atoms and refined. The intramolecular distances proved

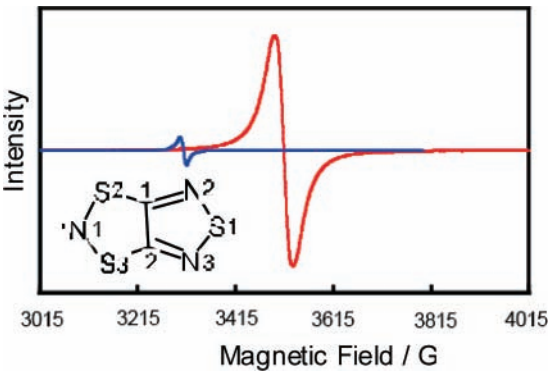

Figure 1. ESR spectra of the HT (red line, 300 K) and LT (blue line, 120 K) phases of polycrystalline 1,3,5-trithia-2,4,6-triazapentalenyl (TTTA) radical, shown with the atom labeling in the inset.

sensitive to the refinement conditions. Because our temperature-resolved single crystal study of TTTA indicated negligible temperature variation of the intramolecular distances, restraints were applied to obtain values that reasonably reproduced the single-crystal values with acceptable fits. The electron densities were calculated and visualized with the maximum entropy method (MEM) using the program PRIMA.[21]

3. Results and Discussion

3.1. Thermally Induced Phase Transition. The thermally induced structural phase transition of TTTA is of first order. From the structures of the two phases, the phase transition has been ascribed[10−12] to reversible dimerization equilibrium, which results in spin coupling and decoupling, and corresponds to a significant change in the magnetic moment between the two phases. If monitored by ESR spectroscopy (Figure 1), cooling of the HT phase is accompanied by a decrease of the strong singlet resonance of the unpaired electron ($g = 2.0048$) because of molecular dimerization and spin pairing. However, it should be noted that a weak residual signal ($g = 2.0048$) remains in the LT phase, even when the sample is cooled far below the transition temperature (*vide infra*). The temperature of the phase transition of microcrystalline sample monitored by ESR generally conforms to the limiting values $T_{\downarrow} = 230$ K on cooling ($\downarrow$) and $T_{\uparrow} = 305$ K on heating ($\uparrow$), on the basis of magnetic susceptibility measurements,[11] and $T_{\downarrow} = 234$ K on cooling and $T_{\uparrow} = 317$ K on heating, on the basis of magnetic measurements and ESR data.[12] The single crystalline samples at ambient pressure showed slightly different values, which seemed to depend on the thermal history of the sample (the temperature at which the sample was stored, application of pressure during grinding, and conditions of the sublimation). One of the reasons behind the slightly different temperatures reported may be the different pressure employed in the experiments; as was shown recently, the pressure affects both the transition temperature and the difference in the magnetic susceptibility between the two phases.[14] Another important reason might be that the powder and single-crystalline samples exhibit slightly different thermal behavior.

The X-ray diffraction experiments on single crystals of TTTA[22] confirmed the previous conclusions that in the HT paramagnetic phase the crystals of TTTA are monoclinic (space group $P2_1/c$) and composed of crystallographically equivalent molecules. Our attempts to obtain high-quality single crystals of the LT phase *in situ*, by cooling single crystals of the HT phase while controlling and monitoring the temperature gradient of the open-flow cooling nitrogen gas, were unsuccessful. During the HT → LT transition, diffraction patterns of single crystals of TTTA, which were obtained as very pure monoclinic (HT) phase by sublimation, indicated increased crystal mosaicity, although the overall crystal integrity was preserved. Replacement of the glue used to fix the crystal with grease in order to avoid eventual additional stress that may be exerted because of the different thermal expansion coefficients of the TTTA crystal and the glue did not result in any improvements.[23] The decreased crystallinity could be improved neither by very slow gradual cooling nor by flash freezing, and this probably represents an inherent structural consequence of the large perturbation taking place during phase transition. The partial loss of crystallinity reflects significant stress exerted on the lattice by structural perturbation. Because the temperature behavior of the powder samples proved to be more reproducible than that of the single crystals, the transition was studied with powder diffraction.

TABLE 1: Lattice Parameters (Å, deg), Selected Intermolecular Distances (Å), and Refinement Statistics of the Three Phases of the 1,3,5-Trithia-2,4,6-triazapentalenyl (TTTA) Radical

T/K	300	280	280	
phase	HT	LT	PI[b]	expected[a]
lattice params.	9.454(31)	7.0010(4)	9.448(2)	
	3.717(12)	7.5061(4)	3.705(1)	
	15.081(49)	10.0173(6)	15.051(3)	
	90	77.570(4)	90	
	104.61(11)	79.356(4)	104.55(2)	
	90	82.983(4)	90	
N1−N1′	3.717(12)		3.705(1)	3.66−3.72[c]
		3.430(11)		3.21−3.28
		3.665(11)		3.86−3.91
S1−S1′	3.717(12)		3.705(1)	3.66−3.72[c]
		3.406(8)		3.46−3.51
		3.848(8)		3.65−3.70
R_p/%	4.02	3.18	2.38[c]	
R_{wp}/%	5.66	5.13	3.66[c]	

[a] Expected from the temperature-averaged single-crystal data for the HT[c] and LT[d] phases. [b] Only the PI component of the binary phase mixture. [c] The reliability factors of the phase mixture are not directly comparable to those of the pure phases because of the different method used to calculate the respective values.

Because it was noticed that both the grinding method and prolonged aging of the TTTA crystals affect their phase purity, only freshly sublimed and powdered TTTA crystals, synthesized by the modification of the previously published procedure,[10] were used in the experiments. The powder diffraction pattern was recorded in Debye−Scherrer geometry using monochromatic synchrotron X-rays with $\lambda = 0.6358$ Å. The refined lattice parameters and intracolumnar separations are listed in Table 1. At 300 K (Figure 2), the pattern conforms to the structure of the pure HT phase (monoclinic, $P2_1/c$) calculated from the fractional coordinates from the single-crystal data. The lattice parameters at 300 K refined from the powder data ($a = 9.454(31)$, $b = 3.717(12)$, $c = 15.081(49)$ Å, and $\beta = 104.61(11)°$) agree very well with the reported single-crystal values[10−12] (e.g., $a = 9.4430(8)$, $b = 3.7170(4)$, $c = 15.0630(8)$ Å, and $\beta = 104.615(5)°$ at 310 K reported by Rawson et al.[12]) and with our single-crystal data at 280 K.[22] Rietveld refinement of the atomic coordinates confirmed that in the HT structure the planar TTTA molecules form $\pi-\pi$-stacked columns with an *aaaa* packing pattern and an intramolecular separation of 3.717(12), which corresponds to the length of the *b*-axis (Figure 6).

When cooled, the lattice of the HT phase shrinks, which becomes apparent in the shift of the reflections toward higher

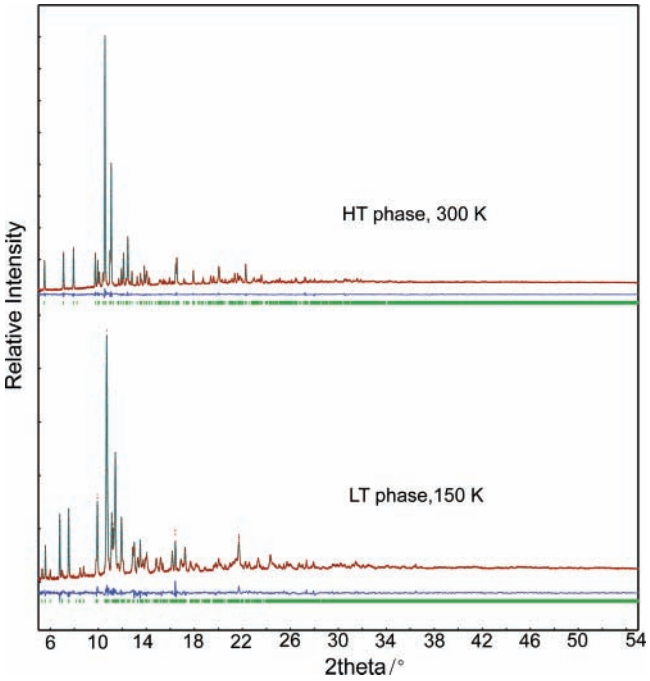

Figure 2. Experimental (red line) and fitted (green line) powder diffraction patterns and their difference (blue line) of the HT phase at 300 K (top; $R_{wp} = 5.66\%$, $R_p = 4.02\%$) and the LT phase at 150 K (bottom; $R_{wp} = 5.34\%$, $R_p = 3.58\%$) of the 1,3,5-trithia-2,4,6-triazapentalenyl (TTTA) radical.

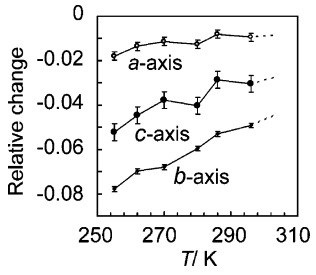

Figure 3. Thermal profile of the absolute changes of the unit cell axes (in Å) in the HT phase relative to ambient temperature values ($a = 9.4364$, $b = 3.7226$, and $c = 15.0479$ Å) as refined from a limited number of reflections collected from a single crystal of the 1,3,5-trithia-2,4,6-triazapentalenyl (TTTA) radical. The temperatures are corrected for differences between the monitored temperature and the real temperature measured independently at the sample position.

2Θ angles. In the HT regime, the thermal shortening of the cell axes (refined from single-crystal data) on cooling is anisotropic and most pronounced along the stacking direction, parallel to the *b*-axis. The decrease of intermolecular separation with only subsidiary changes in the intercolumnar interactions is probably the crucial feature that triggers dimerization. Cooling from 250 K down to 100 K results in the appearance of new peaks from the LT phase in the powder diffraction pattern, which is consistent with lowering of the crystal symmetry (Figures 2 and 4). Particularly, the appearance of the reflections (001), (100), (101), (110), (102) and $(\bar{1}\bar{1}1)$ of the LT phase in regions that are transparent to peaks from the HT phase (2Θ values of 3.75, 5.37, 6.04, 7.03, 8.54, and 8.84°, respectively) represents clear evidence of the structural transformation.

The structure of the LT phase was refined from the powder diffraction patterns at 150 K (Figure 2) and after heating to 280 K (Figure S1, Supporting Information). At both temperatures, the LT phase is triclinic (space group $P\bar{1}$) and almost completely diamagnetic. In the LT phase, the TTTA molecules form

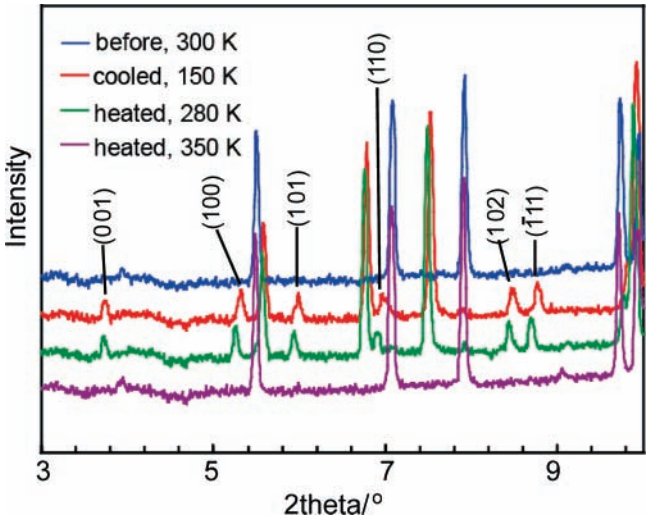

Figure 4. Low 2Θ region in the powder diffraction pattern of the 1,3,5-trithia-2,4,6-triazapentalenyl (TTTA) radical cycled between 300 K (blue, top), 150 K (red), 280 K (green), and 350 K (purple, top). Marked reflections represent selected reflections of the LT phase.

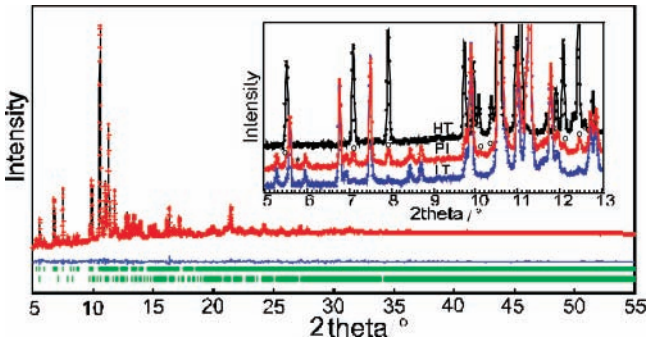

Figure 5. Experimental (red crosses) and fitted (black line) powder diffraction patterns and their difference (blue line) of a binary mixture of the LT phase (upper tickmarks) and PI phase (lower tickmarks) of the 1,3,5-trithia-2,4,6-triazapentalenyl (TTTA) radical. Inset: Low angle region of the diffraction patterns of the high temperature (HT), low temperature (LT), and photoinduced (PI) phases. Peaks of the PI phase are marked with circles. The very weak peak around 5.75o labeled with an asterisk in the inset is present in the pattern of the LT phase, and therefore, it cannot be assigned to a secondary PI phase.

π-stacked dimers with alternating intracolumnar N−N′ distances of 3.430(11) and 3.665(11) A, and S1−S1′ distances of 3.406-(8) and 3.848(8) Å (Figure 6).

The HT and LT structures suggest that similarly to the single-crystalline state, in the powder state the thermal phase transition proceeds through a spin-Peierls (SP) instability-induced reversible $\pi-\pi$ dimerization of the stacked molecules. The decrease of crystallinity in the case of the transition of cooled TTTA single crystals can be rationalized by the significant difference in the crystal structures of the two phases. Upon the phase change, the $\pi-\pi$ stacked molecules of the HT phase are rearranged and realigned into dimers, which requires inclination of the individual TTTA molecules relative to their initial orientation. Because of the strong molecular coupling, the reorientation exerts anisotropic distribution of the internal pressure in the crystal, which affects the long-range order, ultimately resulting in the creation of crystal domains with slightly different molecular orientations. The most probable explanation for the wide hysteresis gap of the transition is energetic quasidegeneracy of the two lattices and the low-energy barrier for their interconversion.

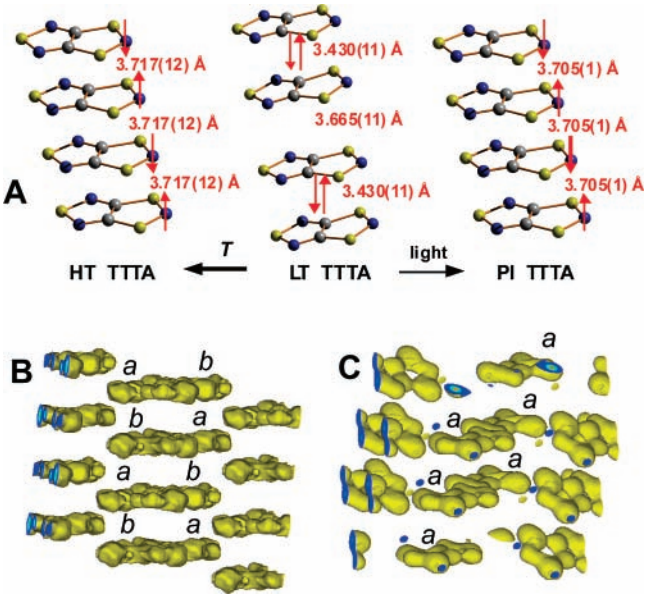

Figure 6. (A) Structural variations within the 1,3,5-trithia-2,4,6-triazapentalenyl (TTTA) crystal due to thermally induced or photoinduced phase transitions according to the Rietveld refinement. The values represent the N1−N1′ distances according to the labels in Figure 1. (B) and (C) represent the maximum entropy method-based electron density plots of the LT and PI phases, respectively (1 e·A^{-3} isosurfaces).

An important experimental observation is the very small amount of residual HT phase, which remains untransformed to the LT phase even at temperatures that are much lower than the lower temperature limit of the HT → LT phase transition. In order to confirm the reproducibility, the thermal transition of TTTA was studied in several experiments on different batches of freshly sublimed samples. The phase purity of the HT phase was always established from the powder diffraction patterns. In all cases, after completion of the HT → LT phase transition, very weak peaks from traces of the residual HT phase were observable (see the pattern of the LT phase in Figure 5), even when the samples were cooled down to 80 K, far below the lower temperature limit of the transition. The traces of the residual HT phase appear as a residual resonance shifted to the low-field side in the LT ESR spectrum (Figure 1). This tiny amount of the HT phase did not increase on heating, and its amount depended on the method used to grind the sample. Therefore, the residual amount of the HT phase is probably due to the permanent lattice strain induced in TTTA crystals by the pressure exerted during grinding. In all experiments, with very careful preparation of the sample under dark conditions, we were able to decrease the residual phase to amounts that are insignificant for the Rietveld refinement.[24]

3.2. Photoinduced Phase Transition. The photoinduced phase transition (PIPT) of TTTA was studied with a setup for steady-state powder photodiffraction, in which a pumped laser source for excitation of the sample was combined with synchrotron X-ray for probing the structural change. For this purpose, 4−6 ns 10 Hz pulses of a Nd:YAG source were coupled in a quasiparallel geometry with monochromated X-rays (λ = 0.6358 Å), an image plate detector, and an open-flow nitrogen low-temperature system. The sample area probed by the X-rays in Debye−Scherrer mode was uniformly excited using unfocused laser radiation with a round spot profile of area 16.4 mm^2. Samples of freshly sublimed and powdered TTTA crystals were used. As described above, at 150 K, TTTA was almost completely converted to the dimerized state of the triclinic LT phase, which remained unchanged on heating to 280 K. Irradiation[25] of the LT phase at 280 K with 355 nm pulses did not affect the diffraction pattern, even upon prolonged irradiation with increasing energy. However, excitation with the 532 nm laser using 10 Hz pulses of 11.3(6) mJ of energy during the 5-s exposure to the X-ray probe resulted in the appearance of new peaks, corresponding to the PI phase, at positions identical to those of the strong peaks of the HT phase (Figure 5). The excitation wavelength of 532 nm is close to the 590 nm band of the LT phase[16] and mostly excites the *inter*dimer charge-transfer transition of the TTTA dimers. Further irradiation did not change the LT/PI ratio, confirming that the maximum active volume of the sample was converted. This mixture of LT and PI phases was stable in the dark at 280 K, but it was converted completely to the pure HT phase by annealing at 350 K, above the upper phase-transition point. The relaxation of both the LT and PI phases to the HT phase confirms the thermal reversibility of the transition and the absence of radiation damage on the time-scale of the experiment.

Structural analysis confirms that during the HT → LT transition, the planar equally spaced $\pi-\pi$ stacked monomeric radical molecules of the HT phase couple into π-stacked dimers of the triclinic LT phase with *abab* packing (Figure 3), which remain unchanged on heating to 280 K. Upon photoexcitation, the dimers of the LT phase are separated, giving the π-stacked radical monomer structure with *aaaa* packing, characteristic of the HT phase (Figure 6). The identical peak positions in the diffraction patterns of the HT and PI phases are unequivocal evidence that their lattice symmetries are indistinguishable. This observation was further confirmed by Rietveld refinement of the atomic positions of the binary LT/PI phase mixture at 280 K after irradiation of the LT phase and of the HT phase obtained by heating of the phase mixture at 350 K. Within the current uncertainties of the refined lattice parameters, the unit cells of the PI and HT phases (509.9(2) Å^3 and 512.8(2.9) Å^3, respectively) are identical, which corresponds with the equal intracolumnar molecular separations of 3.705(1) and 3.717(12) Å (Table 1). (It should be noted that the reliability factors obtained by refinement of the phase mixture are not directly comparable to those of the pure phases because of the different method used to calculate the respective values.)

In our steady-state experiment, we could not identify other (intermediate) photoinduced phases, although the existence of such phases cannot be excluded on shorter time scales. Therefore, the results confirm that the PIPT LT → PI proceeds directly. The thermal stability of the PI phase at 280 K shows that in the case of TTTA, the PIPT process is irreversible. This is contrary to the PIPT observations in some other π-interacting ionic-neutral/monomer−dimer phase equilibria, such as that of the tetrathiafulvalene-chloranil charge-transfer system,[26,27] which probably reflects differences in the mechanisms of the PIPT.

The appearance of new diffraction peaks upon excitation of the LT phase shows that despite the uniform photoexcitation, the photoinduced transition proceeds nonuniformly by the formation of local mesoscopic domains of the new phase, which coexist with the LT phase. The formation of domains is a consequence of the alteration of the long-range order in the crystal, which is brought about by cooperative action by the radical molecules. The photoconversion, as obtained from the peak intensity of the refined fractions of LT and PI phases, is about 14% (by weight) of the PI phase at 280 K. The relatively low conversion during PIPT may be due both to factors intrinsic to the reaction system, such as a small excitation cross-section, or to the experimental setup, where there may be a small active volume because of the limited penetration of light into the

capillary. An additional contribution may have come from the existence of the non-excited LT phase in the interior of the powder particles.

Similar to previous studies of TTTA[16] and other[27−30] systems, heating effects cannot be excluded, although the dependence of PIPT on the excitation wavelength in our photocrystallographic experiments and the spectroscopic results[16] indicate that sample heating is not the primary initiator. Some earlier considerations[31] have pointed out that the high molar concentrations of molecules in small-molecule crystals cause more pronounced laser-induced heating effects relative to macromolecular crystals, where the ensemble of hydration water molecules acts as an effective thermal bath for heat dissipation. The laser-induced heating is a complex result of the action of several experimental factors. The limited penetration depth of the laser because of the high absorption coefficient (dark colored sample) and considerable thickness of the sample ($\leq$0.3 mm) as well as the inherent non-homogeneity and diffusiveness of the laser beam are expected to result in a nonuniform radial profile of the sample laser-heating effects. Although the exposure times were very short (several seconds) in the present experiments, additional effects to heating in the experiment are expected from synchrotron X-rays. In the case of the capillary method, attenuation of laser heating by thermally insulating the capillary is expected to partially counterweigh these effects. Because it is very difficult to measure the absolute temperature within the sample and to separate the individual contributions from various experimental factors, in the present experiments the peak positions of the untransformed LT phase were used as an intrinsic measure of the magnitude of sample heating. The position of diffraction peaks depends on interplanar spacings *d*, which in turn depend on the temperature. Because the PIPT of TTTA proceeds around room temperature, the temperature can be very stably maintained over long periods and can be precisely controlled. At 280 K, sample heating (estimated from the peak shift in 2Θ of $7\cdot10^{-4}$ °/K from the 15 lowest reflections of the LT phase) is 4−5 K, which is close to the value measured with the thermocouple at the sample position and insufficient for the thermal transition LT $\rightarrow$ HT.

4. Conclusions

According to the mechanism of the LT $\leftrightarrow$ HT transition suggested by Okamoto et al.,[16] the LT phase can exist because of the SP instability of the HT phase below the lower transition point. In this study, we achieved direct atomic resolution observation of the formation of mesoscopic domains of TTTA in which SP instability was suppressed by doping with photoinduced charge carriers. The appearance of photoinduced Bragg peaks at positions identical to those of the peaks of the HT phase and the refined structures represents evidence of the identity of the HT and PI phases. These results reveal the nature of the PI phase, and to the best of our knowledge, they represent the first direct evidence for the photoinduced suppression of SP instability in an organic radical crystal. (Photo)diffraction experiments aimed at increasing the accuracy of refined cell parameters and atomic positions of the TTTA phases as well as selective excitation of different electronic transitions of the dimeric structure in the LT phase are now underway.

The results of this study are of much broader significance for research in the fields of structural chemistry and materials science, and particularly for the application of diffraction methods for the direct study of metastable species/states. Namely, two common problems with the X-ray study of photoinduced solid-state processes are the decreased crystallinity and increased mosaicisity in single crystals. In fact, photoinduced reactions/transitions that are characterized by complete preservation of crystal integrity (usually termed single-crystal-to-single-crystal reactions) are very rare among solid-state processes, thus seriously restricting the wider use of single-crystal diffraction for the study of photoinduced solid-state reactions. This obstacle has resulted in only a small number of cases being studied in the past. In the present study, we demonstrate that having the stringent condition of preservation of crystallinity eliminated *a priori*, powder diffraction is a very powerful technique for obtaining direct atomic resolution information about the photoreactions or phase transitions in the solid state.

Acknowledgment. This work is dedicated to Academician Bojan Šoptrajanov, the leader of the Molecular Spectroscopy Group in Macedonia, on the occasion of his 70th birthday. We thank Dr. T. Fujita, Dr. Y. Katsuya, and Mr. D. Nomoto for their help with the X-ray experiments. This study was performed through Special Coordination Funds for Promoting Science and Technology from MEXT of the Japanese Government and through a research grant from the Arai Science and Technology Foundation.

Supporting Information Available: Additional plots of powder diffraction patterns. This material is available free of charge via the Internet at http://pubs.acs.org.

References and Notes

(1) Wolf, S. A.; Awschalom, D. D.; Buhrman, R. A.; Daughton, J. M.; von Molnár, S.; Roukes, M. L.; Chtchelkanova, A. Y.; Treger, D. M. *Science* **2001**, *294*, 1488−1495.

(2) Felser, C.; Fecher, G. H.; Balke, B. *Angew. Chem., Int. Ed*. **2007**, *46*, 668−699.

(3) Pal, S. K.; Itkis, M. E.; Reed, R. W.; Oakley, R. T.; Cordes, A. W.; Tham, F. S.; Siegrist, T.; Haddon, R. C. *J. Am. Chem. Soc*. **2004**, *126*, 1478−1484.

(4) Brusso, J. L.; Clements, O. P.; Haddon, R. C.; Itkis, M. E.; Leitch, A. A.; Oakley, R. T.; Reed, R. W.; Richardson, J. F. *J. Am. Chem. Soc*. **2004**, *126*, 8256−8265.

(5) Brusso, J. L.; Clements, O. P.; Haddon, R. C.; Itkis, M. E.; Leitch, A. A.; Oakley, R. T.; Reed, R. W.; Richardson, J. F. *J. Am. Chem. Soc*. **2004**, *126*, 14692−14693.

(6) Pal, S. K.; Itkis, M. E.; Tham, F. S.; Reed, R. W.; Oakley, R. T.; Haddon, R. C. *Science* **2005**, *309*, 281−284.

(7) Mandal, S. K.; Samanta, S.; Itkis, M. E.; Jensen, D. W.; Reed, R. W.; Oakley, R. T.; Tham, F. S.; Donnadieu, B.; Haddon, R. C. *J. Am. Chem. Soc*. **2006**, *128*, 1982−1994.

(8) Rawson, J. M.; Alberola, A.; Whalley, A. *J. Mater. Chem*. **2006**, *16*, 2560−2575.

(9) Rawson, J. M.; Palacio, F. *Struct. Bonding (Berlin)* **2001**, *100*, 93−128.

(10) Wolmershäuser, G.; Johann, R. *Angew. Chem., Int. Ed*. **1989**, *28*, 920−921.

(11) Fujita, W.; Awaga, K. *Science* **1999**, *286*, 261−262.

(12) McManus, G. D.; Rawson, J. M.; Feeder, N.; van Duijn, J.; McInnes, E. J. L.; Novoa, J. J.; Burriel, R.; Palacio, F.; Oliete, P. *J. Mater. Chem*. **2001**, *11*, 1992−2003.

(13) Fujita, W.; Awaga, K.; Matsuzaki, H.; Okamoto, H. *Phys. Rev. B: Condens. Matter* **2002** *65*, 064434.

(14) Iketaki, K.; Kanai, K.; Tsuboi, K.; Fujita, W.; Awaga, K.; Knupfer, M.; Ouchi, Y.; Seki, K. *Synth. Met*. **2005**, *153*, 457−460.

(15) Tanaka, T.; Fujita, W.; Awaga, K. *Chem. Phys. Lett*. **2004**, *393*, 150−152.

(16) Matsuzaki, H.; Fujita, W.; Awaga, K.; Okamoto, H. *Phys. Rev. Lett*. **2003**, *91*, 017403.

(17) *SAINT−Siemens Area Detector Integration and SMART−Siemens Molecular Analysis Research Tool*; Siemens Analytical X-ray Instruments Inc., Madison, WI, 1996.

(18) Altomare, A.; Cascarano, G.; Giacovazzo, C.; Guagliardi, A.; Burla, M. C.; Polidori, G.; Camalli, M. *J. Appl. Crystallogr*. **1994**, *27*, 435.

(19) Sheldrick, G. M. E. *SHELXL-97*; *Structure Refinement Program*; University of Göttingen: Göttingen, Germany, 1997.

(20) Izumi, F.; Ikeda, T. *Mater. Sci. Forum* **2000**, *321−324*, 198−203.

(21) Izumi, F.; Dilanian, R. A. *Recent Research Developments in Physics*; Part II; Transworld Research Network: Trivandrum, India, 2002; Vol. 3, pp 699−726.

(22) Crystal data at 280 K (corrected temperature): $C_2N_3S_3$, M_r = 162.23, λ = 0.71073 Å, monoclinic, $P2_1/c$, a = 9.4226(10), b = 3.6607(4), c = 15.0233(15) Å, β = 104.517(3) °, V = 501.66(9) Å^3, Z = 4, ρ_{calc} = 2.148 Mg·m^{-3}, μ = 1.338 mm^{-1}, $F(000)$ = 324, Θ range: 2.23 − 33.79°, limiting indices: $-12 \leftarrow h \leftarrow 12$, $-5 \leftarrow k \leftarrow 5$, $-22 \leftarrow l \leftarrow 23$, reflections collected/unique: 6583/1773 (R_{int} = 0.0267), data/restraints/parameters: 1773/0/73, *GoF* = 1.026, final *R* indices [$I > 2\sigma(I)$]: R_1 = 0.0308, wR_2 = 0.0734; *R* indices (all data): R_1 = 0.0586, wR_2 = 0.0899, largest diff. peak/hole: 0.623 / −0.500 e·Å^{-3}. Bond lengths and angles (in Å and deg, the labels refer to the scheme in Figure 1): S(1)−N(3) = 1.6487(17), S(1)−N(2) = 1.6513(16), S(3)−N(1) = 1.658(2), S(3)−C(2) = 1.7331(19), S(2)−N(1) = 1.655(2), S(2)−C(1) = 1.7339(18), N(2)−C(1) = 1.318(2), N(3)−C(2) = 1.320(2), C(2)−C(1) = 1.431(3), N(3)−S(1)−N(2) = 99.26(8), N(1)−S(3)−C(2) = 97.80(9), N(1)−S(2)−C(1) = 98.12(9), C(1)−N(2)−S(1) = 106.02(14), S(2)−N(1)−S(3) = 116.80(10), C(2)−N(3)−S(1) = 106.23(13), N(3)−C(2)−C(1) = 114.04(17), N(3)−C(2)−S(3) = 132.03(15), C(1)−C(2)−S(3) = 113.93(14), N(2)−C(1)−C(2) = 114.45(16), N(2)−C(1)−S(2) = 132.20(15), C(2)−C(1)−S(2) = 113.36(14).

(23) TTTA reacted with some of the epoxy glues that were used; therefore, only nonreactive glue was used in the experiments.

(24) Because the amount remains constant upon heating to the phase transition point, it seems highly unlikely that it can influence the thermal phase transition. Furthermore, it seems highly improbable that the residual phase will influence the photoinduced phase transition. Being structurally and spectroscopically similar to the HT phase, the residual phase should be completely transparent and remain non-excited at the wavelength (532 nm) used for excitation in the photodiffraction experiments.

(25) The light attenuation by the capillary is insignificant because of the small wall thickness.

(26) Koshihara, S.; Takahashi, Y.; Sakai, H.; Luty, T. *J. Phys. Chem.* **1999**, *103*, 2592−2600.

(27) Collet, E.; Lemée-Cailleau, M.-H.; Buron-Le Cointe, M.; Cailleau, H.; Wulff, M.; Luty, T.; Koshihara, S.; Meyer, M.; Toupet, L.; Rabiller, P.; Techert, S. *Science* **2003**, *300*, 612−615.

(28) Hosaka, N.; Tachibana, N.; Shiga, N.; Matsumoto, M.; Tokura, Y. *Phys. Rev. Lett.* **1999**, *82*, 1672−1675.

(29) Koshihara, S.; Tokura, Y.; Takeda, K.; Koda, T. *Phys. Rev. Lett.* **1992**, *68*, 1148−1151.

(30) Chollet, M.; Guerin, L.; Uchida, N.; Fukaya, S.; Shimoda, H.; Ishikawa, T.; Matsuda, K.; Hasegawa, T.; Ota, A.; Yamochi, H.; Saito, G.; Tazaki, R.; Adachi, S.; Koshihara, S. *Science* **2005**, *307*, 86−89.

(31) Moffat, K. *Chem. Rev.* **2001**, *101*, 1569−1581.